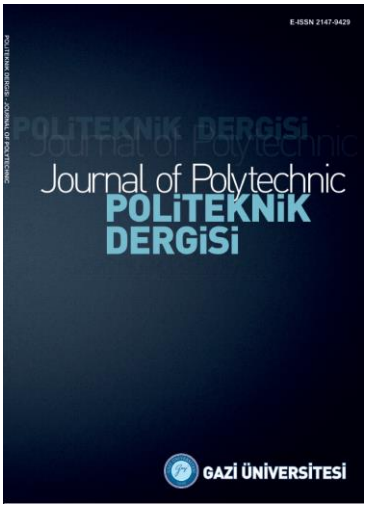

POLİTEKNİK DERGİSİ

JOURNAL of POLYTECHNIC

ISSN: 1302-0900 (PRINT), ISSN: 2147-9429 (ONLINE)
URL: http://dergipark.gov.tr/politeknik

The influence of magnetic field on the growth rate of rayleigh-taylor instability using nano-structured porous linings in inertial confinement fusion fuel targets

Rayleigh-taylor kararsızlığının büyüme hızına manyetik alanın etkisi nano yapılı gözenekli kaplamaların kullanılması eylemsiz hapsedilme füzyon yakıt hedeflerinde

Yazar(lar) (Author(s)): *Arash Malekpour[1], Abbas Ghasemizad[2]*

ORCID[1]: 0000-0003-1148-3872

ORCID[2]: 0000-0001-6452-6309

To cite to this article: Malekpour A. and Ghasemizad A. "The influence of magnetic field on the growth rate of rayleigh-taylor instability using nano-structured porous linings in inertial confinement fusion fuel targets", ***Journal of Polytechnic***, 26(2): 941-951, (2023).

Bu makaleye şu şekilde atıfta bulunabilirsiniz: Malekpour A. and Ghasemizad A. "The influence of magnetic field on the growth rate of rayleigh-taylor instability using nano-structured porous linings in inertial confinement fusion fuel targets", ***Politeknik Dergisi***, 26(2): 941-951, (2023).

Erişim linki (To link to this article): http://dergipark.gov.tr/politeknik/archive

DOI: **10.2339/politeknik.1055366**

The Influence of Magnetic Field on the Growth Rate of Rayleigh-Taylor Instability Using Nano-Structured Porous Linings in Inertial Confinement Fusion Fuel Targets

Highlights

- *The effect of using nano-structured porous linings at the ablation front of ICF fuel targetsis obtained.*
- *The influence of exrting magetic field to the ablative surface of ICF fuel targets is acquired.*
- *The porous parameter is calculated for three different ICF fuel targets.*
- *The growth rate of Rayleigh-Taylor instability as a function of wave number is obtained in each case.*

Graphical Abstract

In this study, decreasing the growth rate of RTI for different ICF fuel targets is investigated by applying nano-structured porous linings at the ablation front of them in the absence and presence of magnetic field.

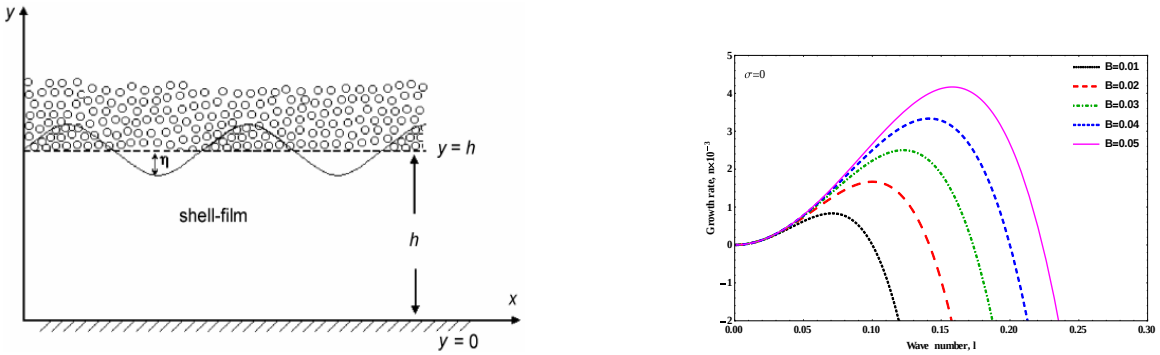

Figure

Aim

The aim of the study is the investigation of the influence of magnetic field on the Rayleigh-Taylor Instability (RTI) growth rate using nano-structured porous linings in Inertial Confinement Fusion (ICF) fuel targets.

Design & Methodology

The equation of RTI growth rate is obtained analytically applying conservation equations, boundary conditions and approximate methods.

Originality

Using nano-structured porous linings at the ablation front of different ICF fuel targets is in good agreement with previous analytical investigations. Also the idea of exerting a powerful magnetic field to the ablative surface of them is a new idea that will be very useful for achieving hydrodynamic stability.

Findings

It is found that higher values of Hartman number will lead to the lower value of RTI growth rate.

Conclusion

Using nano-structured porous lining and exerting a convenient and powerful magnetic field reduce the growth rate of RTI. So they can be considered as positive factors to achieve hydrodynamic stability in ICF reactions.

Declaration of Ethical Standards

The author(s) of this article declare that the materials and methods used in this study do not require ethical committee permission and/or legal-special permission.

The Influence of Magnetic Field on the Growth Rate of Rayleigh-Taylor Instability Using Nano-Structured Porous Linings in Inertial Confinement Fusion Fuel Targets

Araştırma Makalesi / Research Article

Arash Malekpour[1], Abbas Ghasemizad[2*]
[1] Department of Physics, Faculty of Science, University of Guilan, Rasht, Iran
[2] Department of Physics, Faculty of Science, University of Guilan, P.O. Box 1914, Rasht, Iran
(Geliş/Received : 10.01.2022 ; Kabul/Accepted : 03.05.2022 ; Erken Görünüm/Early View : 27.06.2022)

ABSTRACT

In recent years, achieving hydrodynamic stability in inertial confinement fusion (ICF) targets by applying nanostructured porous linings at the ablation front of them has been of particular importance to scientists. Hydrodynamic instabilities, the most significant of which is Rayleigh-Taylor instability (RTI), play a significant role in many physical phenomena. So how to decrease the growth rate of these instabilities is an important purpose in ICF fuel targets. In this research, reducing the growth rate of RTI for various fusion fuel targets has been investigated in two stages: First, it is indicated that applying different nanostructured porous linings at the ablation front of them in the absence of a strong magnetic field causes to decrease RTI growth rate and second, it is shown that using various nanostructured porous linings at the ablation front of these targets accompanying magnetic field exerting to the ablative surface of them, leads to more reduction of RTI growth rate. In both of these two phases, RTI growth rate is acquired analytically using conservation equations, boundary conditions and approximate methods and it is indicated that applying nanostructured porous linings and exerting a powerful magnetic field, will decrease RTI growth rate.

Keywords: Hydrodynamic instability, rayleigh-taylor instability, nano-structured porous lining, growth rate, fuel target.

Rayleigh-Taylor Kararsızlığının Büyüme Hızına Manyetik Alanın Etkisi Nano Yapılı Gözenekli Kaplamaların Kullanılması Eylemsiz Hapsedilme Füzyon Yakıt Hedeflerinde

ÖZ

Son yıllarda, atalet önlerine nanoyapılı gözenekli astarlar uygulayarak eylemsiz hapsetme füzyonu (ICF) hedeflerinde hidrodinamik kararlılığa ulaşmak bilim adamları için özel bir öneme sahip olmuştur. Hidrodinamik kararsızlıklar, en önemlisi Rayleigh-Taylor kararsızlığıdır (RTI), birçok fiziksel olayda önemli bir rol oynar. Böyle, bu istikrarsızlıkların büyüme hızının nasıl düşürüleceği, ICF yakıt hedeflerinde önemli bir amaçtır. Bu çalışmada, RTI büyüme hızının azaltılması çeşitli füzyon yakıtı hedefleri için iki aşamada incelenir: Birinci, güçlü bir manyetik alanın yokluğunda ablasyon önlerine farklı nanoyapılı gözenekli astarların uygulanmasının RTI büyüme hızının azalmasına neden olduğu belirtilmektedir ve ikinci, bu hedeflerin ablatif yüzeyine uygulanan manyetik alana eşlik eden ablasyon cephesinde çeşitli nano yapılı gözenekli astarların kullanılmasının, RTI büyüme hızının daha fazla azalmasına yol açtığı gösterilmiştir. Bu iki fazın her ikisinde de, RTI büyüme hızı, koruma denklemleri, sınır koşulları ve yaklaşık yöntemler kullanılarak analitik olarak elde edilir ve nanoyapılı gözenekli kaplamaların uygulanması ve güçlü bir manyetik alan uygulanmasının RTI büyüme hızını azaltacağı belirtilmektedir.

Anahtar Kelimeler : Hidrodinamik kararsızlık, rayleigh-taylor kararsızlığı, nano yapılı gözenekli astar, büyüme oranı, yakıt hedefi.

1. INTRODUCTION

When a low density fluid accelerates a dense one, or while a heavy fluid placed on a light one in a gravitational field, RTI occurs at the fluid interface and finally generates turbulent mixing of fluids [1]. In this instability which was investigated mathematically by Lord Rayleigh in 1883, the acceleration is preserved. Also G. I. Taylor in 1950 indicated that RTI can occur in accelerated fluids [2]. This instability has many applications in meteorology, astronomy, fluid dynamics and inertial confinement fusion (ICF) [3]. In ICF, to raise the energy gain of fuel pellets, they are constructed in multi-layered spherical shape [4]. The number of fuel layers appertains to the kind of driver (laser or ionic fusion) and the type of driving (direct drive method or indirect drive method)

*Sorumlu Yazar (Corresponding Author)
e-posta : ghasemi@guilan.ac.ir

[5]. In designing these fuel pellets in direct drive method of laser ICF, the central zone is usually composed of low density, high temperature and high entropy DT gas fuel surrounded by a layer containing DT solid fuel with high density, low temperature and low entropy [6]. So, to attain more hydrodynamic efficiency, a low-Z ablator is applied to absorb the energy of the incident laser beams radiated to the outer surface of the fuel pellet [7]. One of the ways achieving this purpose is to investigate the effect of exerting a powerful magnetic field in addition to the accompaniment of a nano-structured porous layer at the ablation front of ICF fuel targets to reduce RTI growth rate. In this situation, both homogeneous incompressible fluid and compressible Boussinesq fluid, which is electrically conductive, are considered to be bounded from the bottom by a solid surface and from the top by a nano-structured porous lining.

Ablator layer contains a foam and is enclosed with a very fine layer consisting of a high-Z material such as gold (Au) and owns a thickness of about 25 nm as the outer layer. When this layer is irradiated by laser pulses, the X-rays generated in the foam layer are symmetrized and preheat the shell before the ablation process begins; as a result, the laser pulses are absorbed in the foam layer with high yield [8]. Even if the gold layer is not applied, since the foam layer has a porous structure, it can uniform and smooth out the in-homogeneities in laser pulses and act as a hohlraum in the indirect drive method [9]. In fact, the pores in the foam layer permit the perturbations to pass through and thus substantially decrease the growth rate of hydrodynamic instabilities. In addition, the pores in the foam layer may deform the expansion and contraction of the flow and cause nonlinear flow. To attain linear flow, a nano-structured porous lattice with very fine pores of nanometer order can be applied. These lattices called nano-structured porous linings, have the capability to remain unchanged due to owning fine pores. Foametal or aloxite are examples of them [10]. Physically, the basic equations for a system including a nano-structured porous lining (which is compacted at high density and saturated with an incompressible viscos fluid) and the shell-film (an incompressible layer which is in contact with the porous lining) consist of momentum and mass conservation equations as follows [10]:

$$\bar{\rho}\frac{\partial \vec{q}}{\partial t} = -\nabla p + \bar{\mu}\nabla^2\vec{q} - \mathrm{K}\,\vec{q} \tag{1}$$

$$\vec{\nabla}.\vec{q} = 0 \tag{2}$$

where $\vec{q} = \vec{q}(u,v)$ is fluid velocity in which u and v are x and y components of its velocity, $\bar{\rho}$ is density, p is fluid pressure in shell-film, $\bar{\mu}$ is viscosity coefficient inside the shell and K is the permeability as follows: global radyasyon ve 9,26 saat güneşlenme süresi ortalama değerlerine sahiptir [1].

$$\bar{\rho} = \rho_f\left[1 + X_p\left(\frac{\rho_p}{\rho_f} - 1\right)\right] \tag{3}$$

$$\bar{\mu} = \mu_f\left[1 + X_p\left(\frac{\mu_{ef}}{\mu_f} - 1\right)\right] \tag{4}$$

$$\mathrm{K} = X_p\left(\frac{\mu_f}{k} + \frac{\rho_p C_b}{\sqrt{k}}|u|\right) \tag{5}$$

where the subscripts f and p specifies shell-film and porous layer, μ_{ef} is effective viscosity, μ_f is the fluid viscosity inside the shell, k is the fluid permeability of porous layer which has the line squared dimension, C_b is the drag coefficient and X_p is a constant as follows:

$$X_p = \begin{cases} 0 & \textit{for shell film} \\ 1 & \textit{for porous lining} \end{cases} \tag{6}$$

In this research a shell-film of thickness h is considered as target with a thin shell filled with a light viscous incompressible fluid limited from above to a nano-structured porous lining with dimensions large enough compared to the thickness h and containing a heavy incompressible viscous saturated fluid and restricted to a rigid surface from below as shown in Fig. 1.

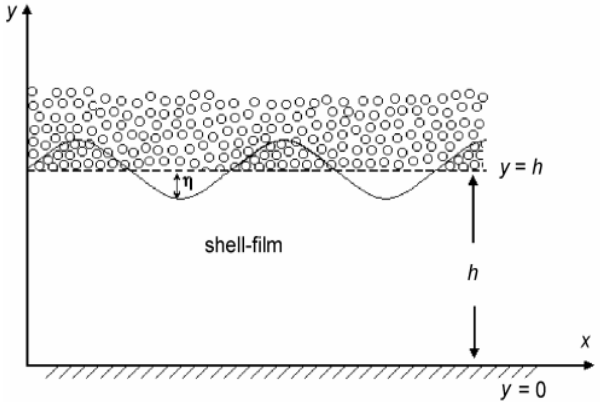

Figure 1. The physical structure of a system consisting of shell film and porous lining [10].

The momentum conservation equation must be solved with appropriate boundary conditions. In this research the analytical computations have been restricted to flows satisfying the Stokes and lubrication approximations [10, 11]:

1. The interface elevation (η) is much smaller than the shell-film thickness (h). By applying this assumption, the variations of u with respect to **x** can be ignored.

2. By assuming $B = \delta h^2 / \gamma << 1$, the gravitational force can be ignored compared to the surface tension; where B is Bond number, $\delta = g\,(\rho_p - \rho_f)$ is the vertical stress, g is the acceleration due to gravity at the fluid interface, ρ_p is the dense fluid constant density in the porous zone, ρ_f is the light fluid density in the shell-film region and γ is the tension of surface.

3. Reynolds number $R = Uh^2 / L\,\nu$, which vouches laminar flow and also internal forces can be ignored with this supposition where $U = \nu / L$ is the characteristic

velocity, $L = \sqrt{\gamma / \delta}$ is the characteristic length and v is the kinematic viscosity.

4. By considering $S = L / T.U << 1$, it can be concluded that the ratio of positional acceleration $(\partial \vec{q} / \partial t)$ to inertial acceleration $((\vec{q}.\vec{\nabla})\vec{q})$ in Equation 1 is insignificant; where S is Strouhal number, $T = \mu\gamma / h^3\delta^2$ is the characteristic time and $\mu = \rho.v$ is the absolute viscosity of fluid.

These approximations permit us to ignore some nonlinear sentences in the momentum conservation equation. We can also assume that due to the approximation of laminar flow in a porous medium compressed with high density, the heavy fluid in the porous lining is almost stationary. So, by applying this supposition, the above mentioned approximations and by using the saffman slip condition, Equations 1 and 2 will be converted as follows [9]:

$$-\frac{\partial p}{\partial x} + \mu_f \frac{\partial^2 u}{\partial y^2} = 0 \tag{7}$$

$$-\frac{\partial p}{\partial y} = 0 \tag{8}$$

Also the incompressibility condition for the x and y components of fluid velocity, u and v respectively, is expressed as the following relation:

$$\frac{\partial u}{\partial x} + \frac{\partial v}{\partial y} = 0 \tag{9}$$

The above equations must be solved by applying convenient surface and boundary conditions, the first of which is the non-slip condition at the solid surface as follows [10]:

$$u = v = 0 \qquad at \quad y = 0 \tag{10}$$

Also, at the interface of porous lining and shell-film, the Saffman slip condition is as follows:

$$\frac{\partial u}{\partial y} = -\frac{\alpha}{\sqrt{k}} u \quad at \quad y = h \tag{11}$$

where α is the slip parameter and k is permeability. In addition to the above conditions, the dynamic and the kinematic conditions at the interface are as follows respectively:

$$p = -\delta\eta - \gamma \frac{\partial^2 \eta}{\partial x^2} \quad at \quad y = h \tag{12}$$

$$v = \frac{\partial \eta}{\partial t} + u \frac{\partial \eta}{\partial x} \qquad at \quad y = h \tag{13}$$

By using linearization, kinematic condition is reduced to the following relation:

$$v = \frac{\partial \eta}{\partial t} \quad at \quad y = h \tag{14}$$

So, by solving Equation 7 applying the boundary conditions mentioned in Equations 10 and 11, the x component of fluid velocity will be acquired as follows:

$$u = \frac{1}{\mu_f} \frac{\partial p}{\partial x} \frac{y}{2}\left(y - \frac{2+\alpha\sigma}{1+\alpha\sigma} \right) h \tag{15}$$

where $\sigma = h / \sqrt{k}$ is porous parameter. By applying scales h for the length, δh for the pressure, $\mu_f / \delta h$ for the time and $\delta h^2 / \mu_f$ for the fluid velocity, the above relations can be expressed as dimensionless equations. So, with these suppositions, Equation 15 can be converted as follows:

$$u = \frac{y}{2}\left[y - \frac{(2+\alpha\sigma)}{(1+\alpha\sigma)} \right] \frac{\partial p}{\partial x} \tag{16}$$

To acquire the y component of fluid velocity, Equation 9 must be integrated from 0 to 1 with respect to y. So by using Equation 16 and after simplification, this component will be obtained as follows:

$$v = -\frac{1}{6}\left(1 - \frac{3(2+\alpha\sigma)}{2(1+\alpha\sigma)} \right) \frac{\partial^2 p}{\partial x^2} \tag{17}$$

2. DISPERSION RELATION LACKING MAGNETIC FIELD

Since Rayleigh-Taylor instability grows exponentially with time, so the amplitude of this instability changes exponentially with time as follows:

$$\eta = \eta_0 \exp(i\ell x + nt) \tag{18}$$

where n is RTI growth rate, ℓ is the wave number and η_0 is initial amplitude of disturbances and in the above equation, the wave vector is considered in the direction of the x-axis. According to Equations 16-18, the dispersion relation has been computed in several steps. In the first step $\partial^2\eta / \partial x^2$ is obtained as follows:

$$\frac{\partial^2 \eta}{\partial x^2} = -\ell^2 \eta_0 \exp(i\ell x + nt) \tag{19}$$

In the second step, by substituting Equation 19 in the relation 12, $\partial^2 p / \partial x^2$ is acquired as follows:

$$\frac{\partial^2 p}{\partial x^2} = \left(-\delta + \gamma \ell^2 \right) \frac{\partial^2 \eta}{\partial x^2} \tag{20}$$

Then in the third step, by combining Equations 19 and 20 and replacing them in Equation 17, the **y** component of fluid velocity is obtained as follows:

$$v = -\frac{1}{6}\left[1 - \frac{3(2+\alpha\sigma)}{2(1+\alpha\sigma)} \right] \left(-\delta \left(1 - \frac{\gamma\ell^2}{\delta} \right) \right) \left(-\ell^2 \eta_0 \exp(i\ell x + nt) \right) \tag{21}$$

On the other hand, in the fourth step, due to Equations 14 and 18, this velocity equals to:

$$v = n\eta_0 \exp(i\ell x + nt) \tag{22}$$

By equating the right side of Equations 21 and 22 and applying the dimensionless relations, the dispersion relation lacking magnetic field is acquired as follows:

$$n=\left[\frac{1}{3}-\frac{\alpha\sigma}{4(1+\alpha\sigma)}\right]\ell^2\left(1-\frac{\ell^2}{B}\right) \quad (23)$$

where n is RTI growth rate and $B = \delta h^2 / \gamma$ is the Bond number. Lacking nano-structured porous layer ($k \to \infty$ or $\sigma \to 0$), Equation 23 converts to the following equation:

$$n_b=\frac{\ell^2}{3}\left(1-\frac{\ell^2}{B}\right) \quad (24)$$

which corresponds to the relation acquired by "Babchin et al. (1983)" [12]. So by applying Equations 23 and 24, the following relation can be expressed as follows:

$$n=n_b-\frac{\alpha\sigma}{4(1+\alpha\sigma)}\ell^2\left(1-\frac{\ell^2}{B}\right)=n_b-\beta\,\ell\,v_a \quad (25)$$

which coincides to the relation acquired by "Takabe et al. (1985)" [13] where:

$$\beta=\frac{3\alpha\sigma}{4+\alpha\sigma} \quad (26)$$

$$v_a=\frac{4+\alpha\sigma}{12(1+\alpha\sigma)}\ell\left(1-\frac{\ell^2}{B}\right) \quad (27)$$

3. RTI GROWTH RATE LACKING MAGNETIC FIELD

In this research, three spherical fuel targets with various amounts of thicknesses (h) have been applied as fusion fuel targets. These fuel targets are presented by "Atzeni et al. (2019)" [14] with h = 870 μm, "Betti and Hurricane (2016)" [15] with h = 422 μm and "Craxton et al. (2015)" [16] with h = 1663 μm. As a result, by applying nano-structured porous layer at the ablation front of them, the changes in RTI growth rate at the ablation front of these fuel targets have been investigated analytically; So that lacking nano-structured porous layer, RTI growth rate is indicated in Fig. 2 for various amounts of Bond number and accompanying it, RTI growth rate can be observed in Figs. 3-10 for the above mentioned fuel targets, different types of these porous layers mentioned in Table 1, α = 0.1 and B=0.04.

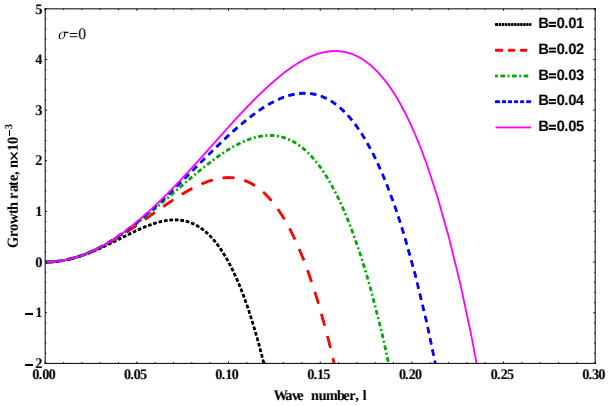

Figure 2. RTI growth rate lacking nano-structured porous lining ($\sigma \to 0$) and magnetic field, for various amounts of Bond number [18].

Table 1. The acquired porous parameters for different nano-structured porous linings applied for various fusion fuel targets [14-17].

Porous Specimens	Permeability k [m^2]	Atzeni's Target		Betti's Target		Craxton's Target	
		h_1 [μm]	σ_1	h_2 [μm]	σ_2	h_3 [μm]	σ_3
Foametal	7.1×10^{-9}	870	10.33	422	5.01	1663	19.74
Foametal A	9.7×10^{-9}	870	8.83	422	4.28	1663	16.89
Foametal C	8.2×10^{-8}	870	3.04	422	1.47	1663	5.81
Aloxite 1	6.45×10^{-10}	870	34.26	422	16.62	1663	65.48
Aloxite 2	1.6×10^{-9}	870	21.75	422	10.55	1663	41.57

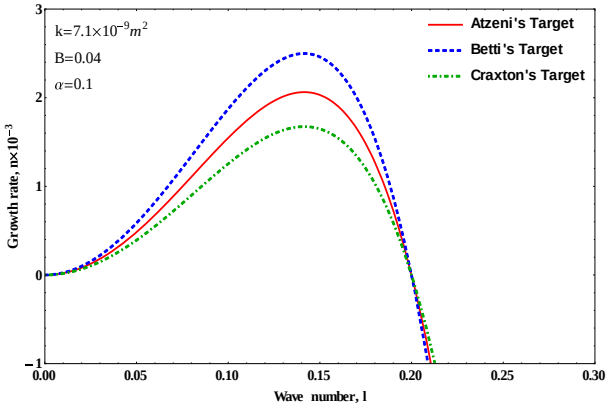

Figure 3. RTI growth rate lacking magnetic field considering $k = 7.1\times10^{-9}\,m^2$

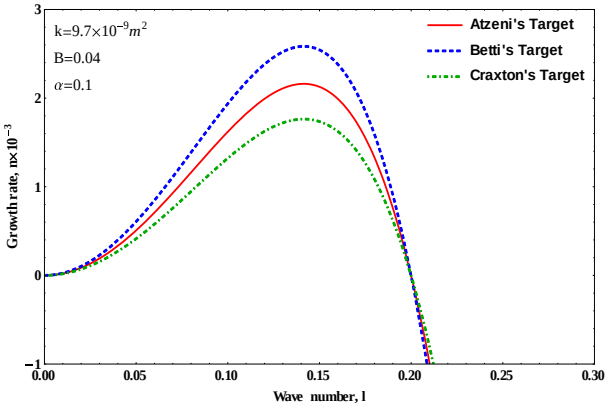

Figure 4. RTI growth rate lacking magnetic field considering $k = 9.7 \times 10^{-9} m^2$

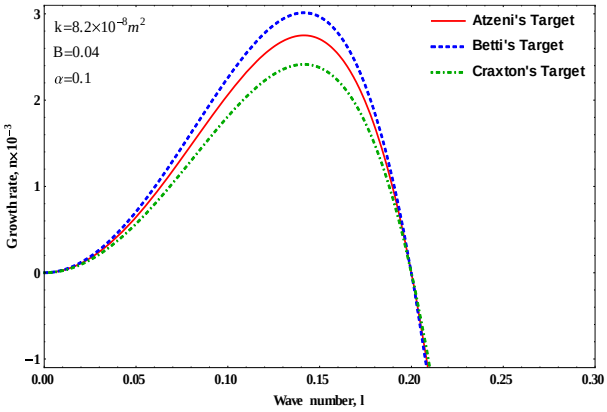

Figure 5. RTI growth rate lacking magnetic field considering $k = 8.2 \times 10^{-8} m^2$

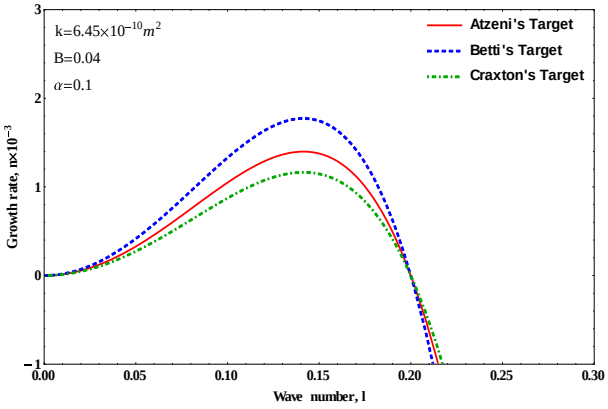

Figure 6. RTI growth rate lacking magnetic field considering $k = 6.45 \times 10^{-10} m^2$

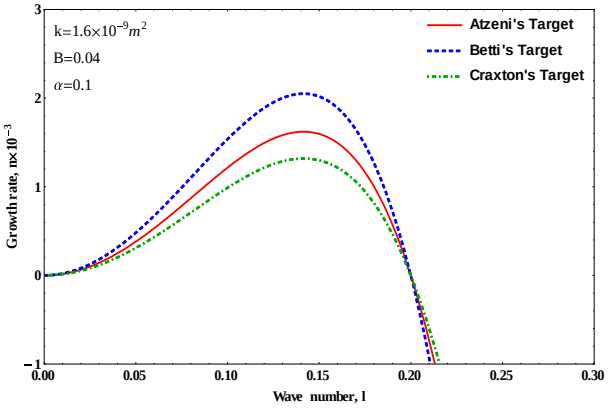

Figure 7. RTI growth rate lacking magnetic field considering $k = 1.6 \times 10^{-9} m^2$

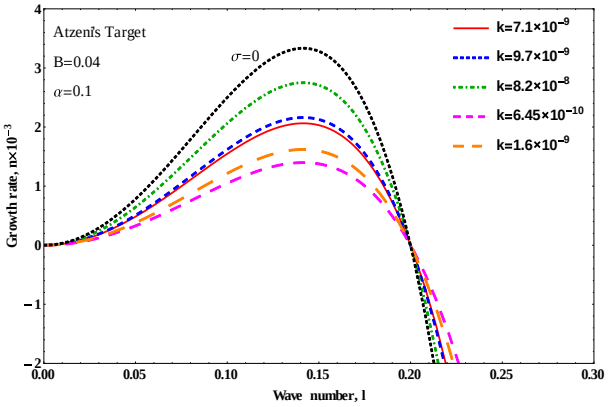

Figure 8. RTI growth rate lacking magnetic field considering Atzeni's Target

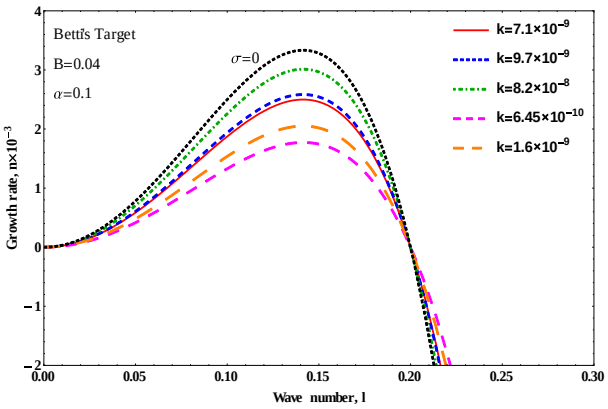

Figure 9. RTI growth rate lacking magnetic field considering Betti's Target

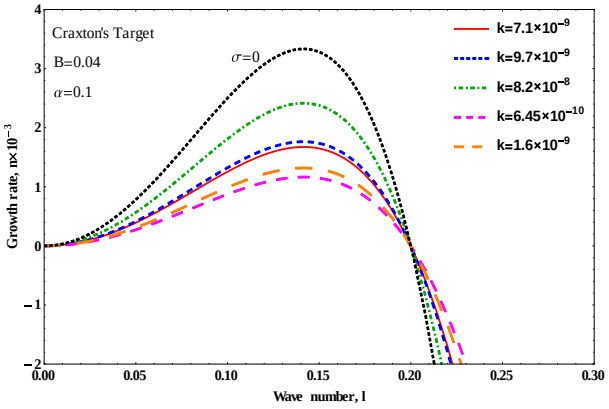

Figure 10. RTI growth rate lacking magnetic field considering Craxton's Target

It can be realized from Fig. 2 that because **γ** is inversely proportional to the Bond number, reducing Bond number amount, increases surface tension. So by decreasing Bond number value, RTI growth rate reduces. It can be understood from Figs. 3-7 that the presence of porous layers decreases RTI growth rate; so that by decreasing the permeability, the growth rate of this instability will reduce too. In other words, as obviously seen in Figs. 8-10, RTI growth rate is proportional to permeability. So, it can be concluded that using the aloxite layers compared to the foametal layers, which have lower permeability, at the ablation front of ICF fuel targets, will make it possible to attain hydrodynamic stability. On the other hand, by applying the fuel targets with appropriate and sufficiently significant thickness, due to their low amount of aspect ratio [19], the growth rate of hydrodynamic instabilities at the interface of them with nano-structured porous linings will decrease more than the other ones. That is why the fuel target presented by "Craxton et al. (2015)" [16] has the lowest value of RTI growth rate compared to the others. This target is very suitable in terms of attaining hydrodynamic stability, so that the performed computations in this research confirm this case.

4. EXERTING MAGNETIC FIELD and MATHEMATICAL COMPUTATIONS

In this case, according to Equation 1, the linear momentum conservation equation due to the addition of the volumetric force expression caused by exerting the magnetic field, called Lorentz force $\bar{\mu}_h \vec{J}\times\vec{H}$ converts to the following equation [20]:

$$\bar{\rho}\left(\frac{\partial \vec{q}}{\partial t}+\left(\vec{q}.\vec{\nabla}\right)\vec{q}\right)=-\vec{\nabla}p+\bar{\mu}_f\nabla^2\vec{q}-K\,\vec{q}+\bar{\mu}_h\,\vec{J}\times\vec{H} \quad (28)$$

The mass conservation equation for a Boussinesq compressible fluid is the same as Equation 2 with the following equation of state:

$$\bar{\rho}=\rho_0\left[1-\alpha_T\left(X_p\left(T_p-T_f\right)+T_f-T_0\right)\right] \quad (29)$$

where X_p is permeability of porous layer, α_T is volumetric expansion coefficient, T_p is temperature of porous layer, T_f is fluid temperature in the shell-film, T_0 and ρ_0 is the temperature and the density of rigid surface respectively. In this case, the energy conservation equation is as follows [20]:

$$(X_p(M'-1)+1)\frac{\partial T}{\partial t}+(\vec{q}.\vec{\nabla})T = (X_p(\kappa'-1)+1)\nabla^2T\pm I_0\,\Omega\,e^{-\Omega y} \quad (30)$$

In Equation 30, $\kappa'=\kappa_{ef}/\kappa$ where κ is thermal diffusivity of fluid, κ_{ef} is the effective thermal diffusivity accompanying porous layer, Ω is absorption coefficient, $M'=\left(\rho c_p\right)_p/\left(\rho c_p\right)_f$ is the heat capacity ratio and the ± sign in the right hand side of this equation, depends on physical condition, videlicet whether energy is lost or gained. Also the current density is as follows:

$$\vec{J}=\bar{\sigma}_h\left[\vec{E}+\bar{\mu}_h\vec{q}\times\vec{H}\right] \quad (31)$$

and Maxwell equations can be expressed as:

$$\vec{\nabla}.\vec{H}=0 \quad (32)$$

$$\vec{\nabla}\times\vec{E}=-\mu\frac{\partial\vec{H}}{\partial t} \quad (33)$$

$$\vec{\nabla}.\vec{E}=0 \quad (34)$$

where magnetic permeability and electrical conductivity are defined respectively as follows:

$$\bar{\mu}_h=\mu_h\left[1+X_p\left(\frac{\mu_p}{\mu_h}-1\right)\right] \quad (35)$$

$$\bar{\sigma}_h=\sigma_p\left[1+X_p\left(\frac{\sigma_{hp}}{\sigma_h}-1\right)\right] \quad (36)$$

and all other quantities in the above mentioned equations have already been introduced.

5. DISPERSION RELATION ACCOMPANYING MAGNETIC FIELD

As the next step, the dispersion relation accompanying a powerful magnetic field exerted to a nano-structured porous lining at the external surface of fuel pellet combined with laser radiation effect has been obtained analytically. By using approximation methods discussed in the previous sections, it can be said that in this situation, Equation 7 converts as follows [20]:

$$-\frac{\partial p}{\partial x}+\frac{\partial^2u}{\partial y^2}-M^2u=0 \quad (37)$$

So that, by solving this differential equation using the boundary conditions mentioned in Equations 10 and 11, the **x** component of fluid velocity is obtained as follows:

$$u=\left\{\frac{M\cosh\left[M\left(1-y\right)\right]+\alpha\sigma\sinh\left[M\left(1-y\right)\right]}{M^{2}\left[M\cosh\left(M\right)+\alpha\sigma\sinh\left(M\right)\right]}+\frac{\alpha\sigma\left[\sinh\left(M\,y\right)-\sinh\left(M\right)\right]-M\cosh\left(M\right)}{M^{2}\left[M\cosh\left(M\right)+\alpha\sigma\sinh\left(M\right)\right]}\right\}\times\frac{\partial p}{\partial x} \quad (38)$$

where $M=\mu H_0 h\sqrt{\sigma_h/\mu_f}$ is Hartman number, H_0 is Magnetization and σ_h is the electrical conductivity. On the other hand, according to Equation 38 the incompressibility condition mentioned in Equation 9 and the boundary conditions mentioned in Equations 10 and 11, the y component of fluid velocity is obtained as follows:

$$v=\left\{\frac{2\alpha\sigma\left[1-\cosh\left(M\right)+M^{2}\cosh\left(M\right)\right]}{M^{3}\left[M\cosh\left(M\right)+\alpha\sigma\sinh\left(M\right)\right]}+\frac{2\alpha\sigma\left[\left(\alpha\sigma-1\right)\times M\sinh\left(M\right)\right]}{M^{3}\left[M\cosh\left(M\right)+\alpha\sigma\sinh\left(M\right)\right]}\right\}\times\frac{\partial^{2}p}{\partial x^{2}} \quad (39)$$

Then, by using the method applied to obtain Equation 25, RTI growth rate accompanying nano-structured porous layer and by exerting magnetic field, can be obtained as follows:

$$n=n_b-\beta\ell v_a \quad (40)$$

where n is RTI growth rate and ℓ is wave number. In above equation, quantities β, v_a and n_b is computed as follows:

$$\beta=\frac{M^{3}-3\left[M-\tanh\left(M\right)\right]}{3\left[M-\tanh\left(M\right)+\alpha\sigma\tanh\left(M\right)+\frac{2\alpha\sigma\left[1-\cosh\left(M\right)\right]}{M\cosh\left(M\right)}\right]}+\frac{\alpha\sigma\left(M^{2}-3\right)\tanh\left(M\right)+\frac{6\alpha\sigma\left[\cosh\left(M\right)-1\right]}{M\cosh\left(M\right)}}{3\left[M-\tanh\left(M\right)+\alpha\sigma\tanh\left(M\right)+\frac{2\alpha\sigma\left[1-\cosh\left(M\right)\right]}{M\cosh\left(M\right)}\right]} \quad (41)$$

$$v_a=\left\{\frac{M-\tanh\left(M\right)+\alpha\sigma\tanh\left(M\right)}{M^{3}\left[1+\alpha\sigma\frac{\tanh\left(M\right)}{M}\right]}+\frac{\frac{2\alpha\sigma\left[1-\cosh\left(M\right)\right]}{M\cosh\left(M\right)}}{M^{3}\left[1+\alpha\sigma\frac{\tanh\left(M\right)}{M}\right]}\right\}\times\ell\left(\delta-\frac{\ell^{2}}{B}\right) \quad (42)$$

$$n_b=\frac{\ell^{2}}{3}\left(\delta-\frac{\ell^{2}}{B}\right) \quad (43)$$

where β is a constant, v_a is the fluid velocity at the external surface of fuel pellet accompanying nano-structured porous lining and by exerting magnetic field, n_b is RTI growth rate lacking magnetic field, which is called RTI growth rate classical value, $B=\delta_0 h^2/\gamma$ is Bond number, δ equals to 1 or $(\theta_{f_1}-\theta_{p_1})$ where $\theta=(T-T_0)/(T_1-T_0)$ is actually dimensionless temperature, θ_f is for $T = T_f$ and about fluid, θ_p is for $T = T_p$ and about nano-structured porous lining, θ_{p_1} and θ_{f_1} are the amounts of θ_p and θ_f at y = 1, the normal stress is $\delta_0=g(\rho_p-\rho_f)$, γ is the surface tension, $\rho_p=\rho_0\left[1-\alpha_T\left(T_p-T_0\right)\right]$, $\rho_f=\rho_0\left[1-\alpha_T\left(T_f-T_0\right)\right]$ and subscript 0 refers to solid surface at y = 0. When $M \to 0$, Equation 40 converts to Equation 25 and lacking nano-structured porous layer ($\sigma \to 0$ *or* $k \to \infty$), Equations 41 and 42 will become the following relation [20]:

$$\beta=\frac{M^{3}-3\left[M-\tanh\left(M\right)\right]}{3\left[M-\tanh\left(M\right)\right]} \quad (44)$$

$$v_a=\frac{\left[M-\tanh\left(M\right)\right]\ell\left(\delta-\ell^{2}/B\right)}{M^{3}} \quad (45)$$

6. RTI GROWTH RATE IN THE PRESENCE OF MAGNETIC FIELD

As the final step, RTI growth rate accompanying magnetic field is investigated for the targets mentioned in the previous section. In this research, nano-structured porous layers assigned in Table 1 have been applied and magnetic field exertion effect is assumed for each of them. So, by using Equation 40, RTI growth rate accompanying magnetic field has been investigated at the ablation front of these targets and in all cases the used magnetic field is uniform and normal to surface of them. RTI growth rate accompanying magnetic field can be seen in Figs. 11-18 for the above noted targets and various types of nano-structured porous linings mentioned in Table 1 and α = 0.1, B=0.04 and M = 1.

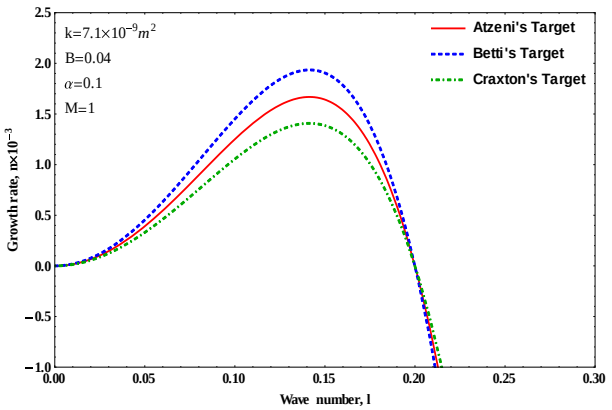

Figure 11. RTI growth rate accompanying magnetic field considering $k=7.1\times10^{-9}m^2$

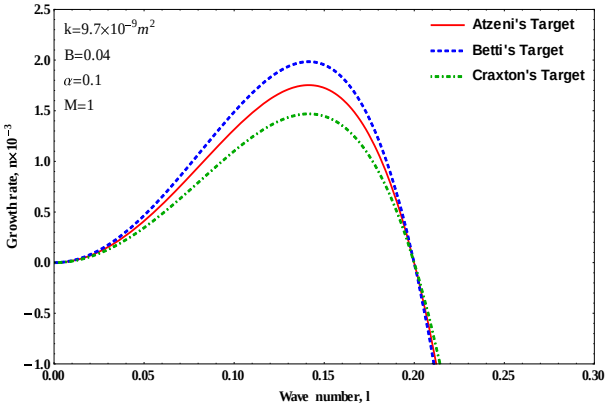

Figure 12. RTI growth rate accompanying magnetic field considering $k = 9.7 \times 10^{-9} m^2$

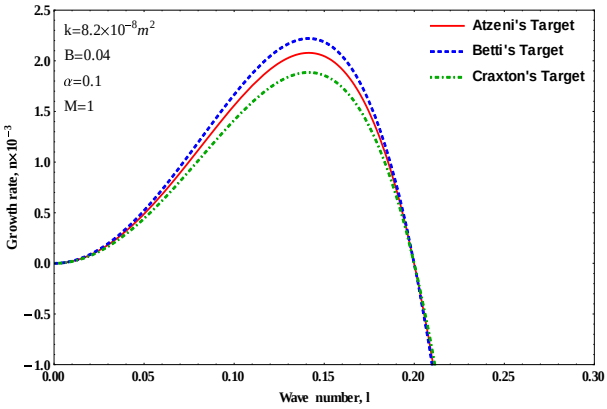

Figure 13. RTI growth rate accompanying magnetic field considering $k = 8.2 \times 10^{-8} m^2$

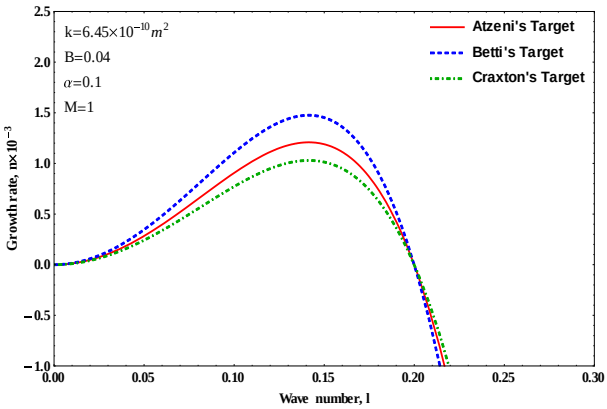

Figure 14. RTI growth rate accompanying magnetic field considering $k = 6.45 \times 10^{-10} m^2$

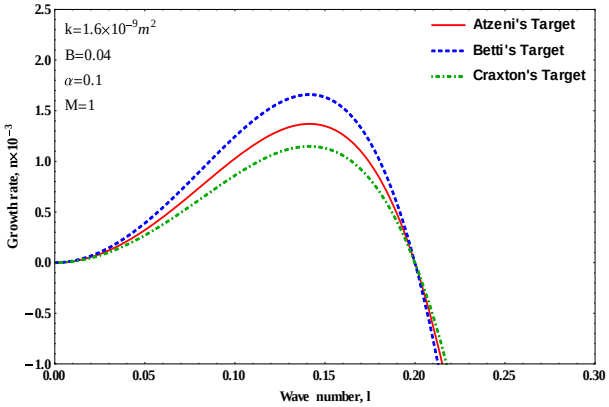

Figure 15. RTI growth rate accompanying magnetic field considering $k = 1.6 \times 10^{-9} m^2$

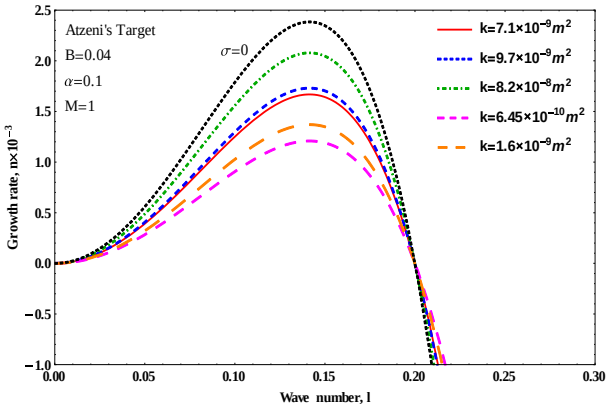

Figure 16. RTI growth rate accompanying magnetic field considering Atzeni's Target

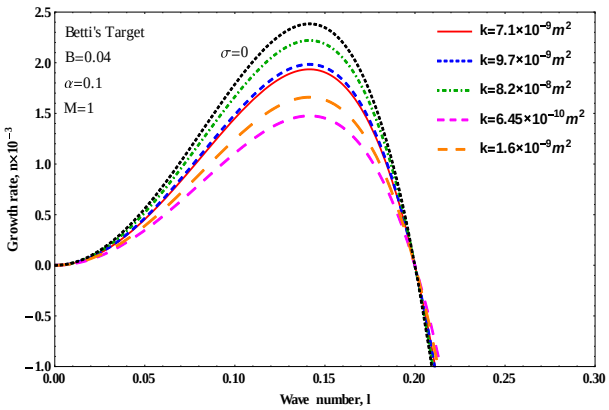

Figure 17. RTI growth rate accompanying magnetic field considering Betti's Target

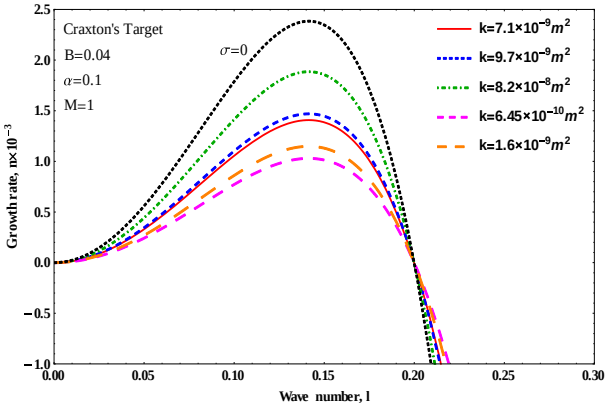

Figure 18. RTI growth rate accompanying magnetic field considering Craxton's Target

It can be derived from Figs. 11-18 compared to Figs. 3-10 that exerting magnetic field to a nano-structured porous lining used in ablation front of a fuel pellet, reduces RTI growth rate. Also, for a particular amount of Bond number, the lower value of permeability leads to the lower amount of RTI growth rate. In other words, it can be deduced that RTI growth rate is directly proportional to permeability. As a result, the target presented by "Craxton et al. (2015)" [16] which is the thickest target with respect to the others, has the least amount of growth rate compared to the others. Therefore, the computations performed in this research confirm that this target is very convenient for attaining hydrodynamic stability. In addition, as indicated in Figs. 19-23, by increasing the amount of Hartman number, the magnetic field becomes more powerful and as a result the growth rate of RTI reduces for each of the above mentioned ICF fuel targets.

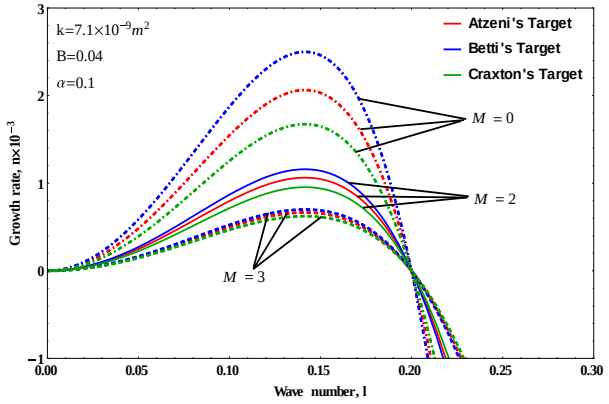

Figure 19. RTI growth rate accompanying and lacking magnetic field and Porous lining considering $k = 7.1\times10^{-9}m^2$

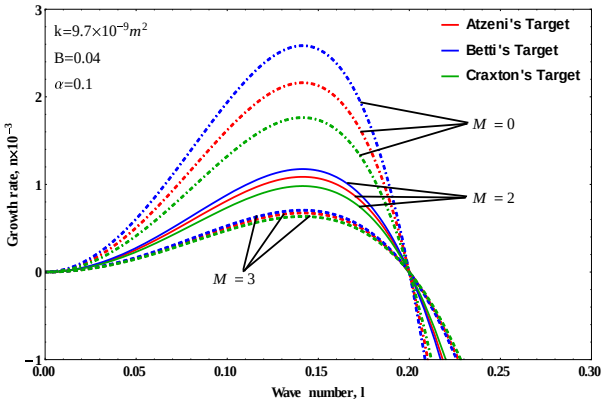

Figure 20. RTI growth rate accompanying and lacking magnetic field and Porous lining considering $k = 9.7\times10^{-9}m^2$

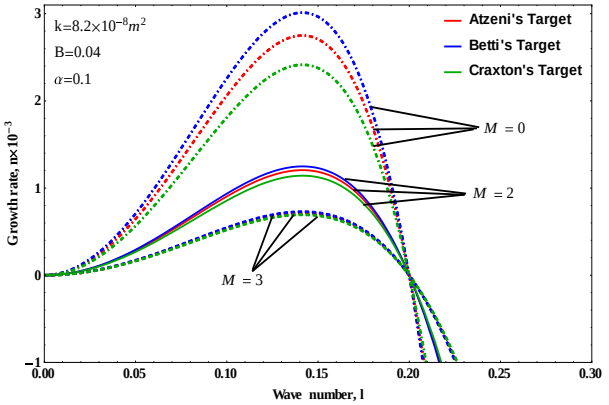

Figure 21. RTI growth rate accompanying and lacking magnetic field and Porous lining considering $k = 8.2\times10^{-8}m^2$

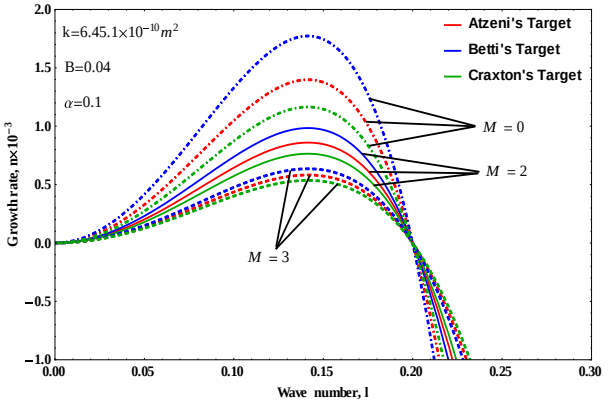

Figure 22. RTI growth rate accompanying and lacking magnetic field and Porous lining considering $k = 6.45\times10^{-10}m^2$

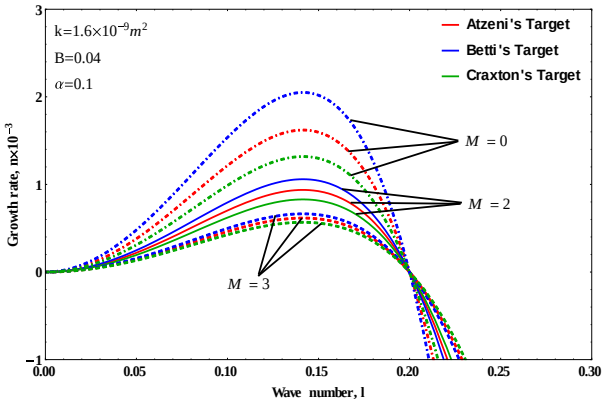

Figure 23. RTI growth rate accompanying and lacking magnetic field and Porous lining considering $k = 1.6 \times 10^{-9} m^2$

Figs. 19-23 show that exerting a magnetic field can substantially reduce RTI growth rate. Also Hartman number illustrates the field's strength; so that the stronger magnetic field and the greater its magnitude indicates the more the value of Hartman number. These figures show that as the magnetic field intensifies and becomes stronger, the growth rate of RTI reduces further. Therefore, it can be derived that because exerting a strong magnetic field with considerable and convenient magnitude decreases the growth rate of RTI, so it can be assumed as a positive factor to attain the hydrodynamic stability.

7. CONCLUSIONS

In this research, RTI growth rate at the ablation front of different fuel targets with various thicknesses is investigated in two stages: In the first stage, applying different nano-structured porous linings with various porous parameters in the ablation front of them to decrease RTI growth rate is investigated; so that solving mass and linear momentum conservation equations, using boundary conditions and approximation methods and acquiring the dispersion relation, the equation related to the growth rate of RTI is acquired analytically . Therefore, it is found that using nano-structured porous layer at the external surface of fuel pellet, will further decrease RTI growth rate compared to its classical value; so that RTI growth rate is proportional to layer's permeability. As a result, it can be derived that applying aloxite layers compared to foametal layers, which have lower permeability, at the ablation front of ICF fuel targets is more suitable. Also the targets with convenient and sufficiently substantial thickness, due to their low value of aspect ratio, are appropriate; because the reduction amount of the RTI growth rate in them, is more than the others. In the second stage, exerting a magnetic field to a nano-structured porous lining used in the ablation front of a fuel target is investigated and it is derived that using a strong magnetic field with high amounts of Hartman number can significantly decrease RTI growth rate, so that Hartman number higher amounts will lead to the lower value of RTI growth rate. So, by applying nano-structured porous lining at the ablation front of ICF fuel targets and by exerting an appropriate magnetic field to the external surface of them, the growth rate of RTI will be substantially decreased and for this reason they can be considered as positive factors to attain hydrodynamic stability in ICF reactions.

ACKNOWLEDGEMENT

This study was conducted as a product of the doctoral thesis prepared.

DECLARATION OF ETHICAL STANDARDS

The author(s) of this article declare that the materials and methods used in this study do not require ethical committee permission and/or legal-special permission.

AUTHORS' CONTRIBUTIONS

Arash Malekpour: Performed the material identification and adjustment, data collection and analysis and wrote the first draft of the manuscript.

Prof. Dr. Abbas Ghasemizad: Reviewed and commented on previous versions of the manuscript.

CONFLICT OF INTEREST

There is no conflict of interest in this study.

REFERENCES

[1] Abarzhi S. I., Nishihara K. and Glimm J., "Rayleigh-Taylor and Richtmyer-Meshkov instabilities for fluids with a finite density ratio", ***Physics Letters A***, 317, 470 (2003).

[2] Piriz A. R., Cortázar O. D., López Cela J. J. and Tahir N. A., "The Rayleigh-Taylor instability", ***American Journal of Physics***, 74, 1095 (2006).

[3] Atzeni S. and Temporal M., "Mechanism of growth reduction of the deceleration-phase ablative Rayleigh-Taylor instability", ***Physical Review E***, 67, 057401 (2003).

[4] Basko M. M., "High gain DT targets for heavy ion beam fusion", Nucl. Fusion 32, 1515 (1992).

[5] Pfalzner S., "An Introduction to Inertial Confinement Fusion", Taylor & Francis, CRC Press, New York (2006).

[6] Moses E. I., "Ignition on the National Ignition Facility: A Path towards Inertial Fusion Energy", ***Nuclear Fusion***, 49, 104022 (2009).

[7] Lafon M., Betti R., Anderson K. S., Collins T. J. B., Epstein R., McKenty P. W., Myatt J. F., Shvydky A. and Skupsky S., "Direct-drive–ignition designs with mid-Z ablators", ***Physics of Plasmas***, 22, 032703 (2015).

[8] Gibbon P. and Förster E., "Short-pulse laser–plasma interactions", ***Plasma Physics and Controlled Fusion***, 38, 769 (1996).

[9] Atzeni S. and Meyer-ter-Vehn J., "The Physics of Inertial Fusion: Beam Plasma Interaction, Hydrodynamics, Hot

Dense Matter", International Series of Monographs on Physics, Clarendon, Oxford (2004).

[10] Rudraiah N., "Effect of Porous Lining on Reducing the Growth Rate of Raleigh-Taylor Instability in the Inertial Fusion Energy Target", ***Fusion Science and Technology***, 43, 307 (2003).

[11] Banerjee R., Mandal L., Roy S., Khan M. and Gupta M. R., "Combined effect of viscosity and vorticity on single mode Rayleigh-Taylor instability bubble growth", ***Physics of Plasmas***, 18, 022109 (2011).

[12] Babchin A. J., Frenkel A. L., Levich B. G. and Shivashinsky G. I., "Nonlinear saturation of Rayleigh-Taylor instability in thin films", ***Physics of Fluids***, 26, 3159 (1983).

[13] Takabe H., Mima K., Montierth L. and Morse R. L., "Self consistent growth rate of the Rayleigh-Taylor instability in an ablatively accelerating plasma", ***Physics of Fluids***, 28, 3676 (1985).

[14] Atzeni S., Schiavi A., Antonelli L. and Serpi A., "Hydrodynamic studies of high gain shock ignition targets: effect of low- to intermediate-mode asymmetries", ***European Physical Journal D***, 73: 243 (2019).

[15] Betti R. and Hurricane O. A., "Inertial-confinement fusion with lasers", ***Nature Physics***, 12, 435 (2016).

[16] Craxton R. S., Anderson K. S., Boehly T. R., Goncharov V. N., Harding D. R., Knauer J. P., McCrory R. L., McKenty P. W., Meyerhofer D. D., Myatt J. F., Schmitt A. J., Sethian J. D., Short R. W., Skupsky S., Theobald W., Kruer W. L., Tanaka K., Betti R., Collins T. J. B., Delettrez J. A., Hu S. X., Marozas J. A., Maximov A. V., Michel D. T.,Radha P. B., Regan S. P., Sangster T. C., Seka W., Solodov A. A., Soures J. M., Stoeckl C. and Zuegel J. D., "Direct-drive inertial confinement fusion: A review", ***Physics of Plasmas***, 22(11): 110501 1-153 (2015).

[17] Goyeau B., Lhuillier D., Gobin D. and Velarde M. G., "Momentum transport at a fluid-porous interface", ***International Journal of Heat and Mass Transfer***, 46, 4071 (2003).

[18] Rahimi Shamami S., Ghasemizad A., "Reduction of growth rate of Rayleigh-Taylor instability using nano-structured porous lining at ICF target shell", ***The European Physical Journal Plus***, 128: 141 (2013).

[19] Schmitt A. J., Bates J. W., Obenschain S. P., Zalesak S. T. and Fyfe D. E., "Shock ignition target design for inertial fusion energy", ***Physics of Plasmas***, 17, 042701 (2010).

[20] Rudraiah N., Krishnamurthy B. S., Jalaja A. S. and Desai T., "Effect of a magnetic field on the growth rate of the Rayleigh–Taylor instability of a laser-accelerated thin ablative surface", ***Laser and Particle Beams***, 22, 29 (2004).